

Shear-induced structural changes of a smectic-A phase: A computer simulation study

G. R. Luckhurst and G. Saielli*

Department of Chemistry and Southampton Liquid Crystal Institute, University of Southampton, Southampton SO17 1BJ, United Kingdom

T. J. Sluckin

Faculty of Mathematical Studies and Southampton Liquid Crystal Institute, University of Southampton, Southampton SO17 1BJ, United Kingdom

(Received 13 August 2001; published 11 April 2002)

We have carried out a Monte Carlo simulation of a thin sample of the smectic-A phase of the Gay-Berne mesogen GB(4.4,20.0,1,1) sandwiched between two plates and subject to shear. The smectic layers are perpendicular to the confining plates and are pinned at the boundaries. The thickness of the samples studied ranges from about three to twenty molecules. The layers tilt progressively with increasing shear, but rearrange themselves at a critical shear. At this critical shear the layers melt near the center of the sample and reform with a reduced tilt consistent with the layer pinning at the walls. The pseudodynamics of this process as the smectic layers melt and are reformed have been followed during the simulation. The critical layer tilt at which slippage takes place tends to a constant value for thick samples, but for very thin samples the critical shear tends toward half a smectic layer, with a significantly reduced translational order near the sample center just before the critical shear. The simulation results are consistent with the predictions of the mean field theory of this phenomenon developed by Mottram *et al.*

DOI: 10.1103/PhysRevE.65.041717

PACS number(s): 61.30.Cz, 61.30.Gd, 61.30.Hn

I. INTRODUCTION

The liquid crystalline smectic-A phase exhibits order intermediate between that of a solid and a liquid [1]. Like all liquid crystals it possesses long range orientational order but its defining quality is the existence of one-dimensional positional ordering in the form of a periodic density function; this is commonly referred to as a layered structure. In equilibrium the layers, for the unconstrained liquid crystal, are uniformly separated by a distance $d=2\pi/q$, where q is the preferred wave number of the density fluctuations. In this paper we use the Monte Carlo simulation technique to study a liquid crystal sample in which the smectic layering is disturbed by an imposed shear field. We consider a smectic-A liquid crystal sample subject to boundary conditions that align the director in the same uniform \hat{x} direction on each surface of the cell. The cell surfaces are parallel to the x - y plane as shown in Fig. 1. These uniform planar boundary conditions, combined with the pinning of the layers, cause the smectic layers to form a bookshelf structure, in the x - z plane [see Fig. 1(a)]. This bookshelf configuration is then disturbed by moving, that is shearing, one boundary plate of the sample with respect to the other, in a direction parallel to the easy axis [see Fig. 1(b)].

A theory of the influence of shear on such a smectic-A sample has been developed by one of us in collaboration with Mottram *et al.* [2] building on a quasistatic Landau-de

Gennes theory proposed by Elston and Towler [3]. The background to the problem is as follows. Phenomenological theories of smectic structures close to surfaces and in thin films typically assume that there exists a surface memory effect that anchors the layers at the cell surfaces while the natural layer spacing may change in the bulk of the cell. The memory effect idea is included implicitly in theories of chevron structure in the technologically important case of ferroelectric liquid crystal cells, in which the bookshelf structure deforms into a V-like layer configuration [4,5]. The degree of anchoring has been measured, albeit inconclusively, by Cagnon and Durand [6]. The formal microscopic basis for this anchoring is poorly understood. It could result from the existence of an easy axis in the surface that gives the director a unique direction that, combined with interactions between the mesogenic molecules that stabilize the side-by-side arrangement, create a layered structure for a monolayer at the surface. The memory effect-induced anchoring is also expected to be important when smectic cells are subject to shear. As we have discussed, the bookshelf layer structure is then distorted in order to maintain the surface layer anchoring. There is consequently a competition between the energetically favorable bookshelf geometry and the applied shear stress.

The theoretical predictions are as follows. With increasing relative shear between the two faces of the sample, there is a complex structure of stable, metastable, and unstable states. The zero-shear situation starts with the smectic layers perpendicular to the boundary plates (see Fig. 1). As the sample is sheared, the layers are progressively tilted. Eventually this tilt can mean that the total degree of shear across the sample corresponds to many smectic layers. Evidently a lower free energy state consistent with the strong anchoring boundary conditions could be achieved by melting the sample and re-

*Corresponding author. Present address: Centro Meccanismi Reazioni Organiche del CNR e Dipartimento di Chimica Organica, Via Marzolo, 1, 35131 Padova, Italy.
Email address: giacomo.saielli@unipd.it

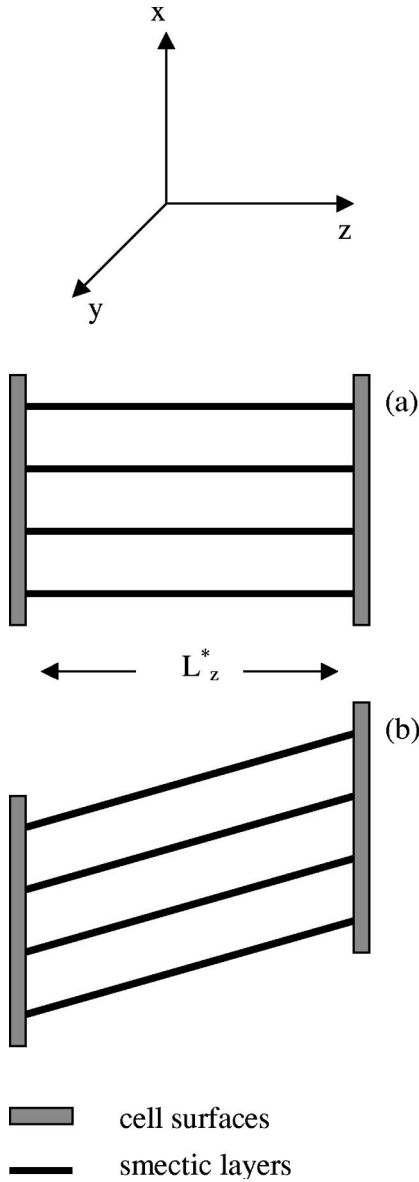


FIG. 1. The configuration of the smectic-A phase in the bookshelf geometry within the parallel plate cell (a) before and (b) after shear, together with the axis system used.

forming the layers so that they tilt less. Here the term *melt*, which is commonly used in this field of liquid crystals, means that the translational order for the smectic phase has decreased to zero, although the orientational order does not necessarily vanish. The lowest energy state occurs when the tilt corresponds to a relative displacement across the cell of less than half a smectic layer. The metastable state that is reached by tilting the layers by shearing the cell for greater displacements is known as a *supersheared* state.

The theory predicts that under most circumstances there is significant supershear, but that for sufficiently large shear, corresponding to a large tilt, the metastable supersheared state becomes unstable. When this instability occurs, the layers melt in the center of the sample, and they reform in such a way that the degree of shear is just one smectic layer less than it had been when the limit of stability had been reached.

For very thin samples the theory predicts that at the limit of stability (a) the degree of smectic order at the center of the cell will be reduced, and (b) the total tilt will be greater than for thick samples.

Finally, it is predicted that there is a minimum cell thickness, normally of molecular dimensions, below which supershear does not take place under an increasing shear. Now, as the shear is increased from zero the degree of translational order in the center of the cell is reduced. When the shear is exactly half a layer thickness, the layers melt in the center of the sample. If the shear is made arbitrarily larger than this quantity, the layers reform, now with the opposite tilt. With further shear, the layers straighten up again, so that when the shear is exactly one smectic layer, the layers are restored to their original unperturbed or orthogonal state.

In order to explore the behavior of a thin layer of a smectic-A phase under shear and hence the validity of the mean field theory developed to describe the problem, we have undertaken a Monte Carlo computer simulation study. This approach has the advantage that we can investigate a model system consistent with that on which the theory is based, in particular, with the layer pinning at the cell surfaces. In addition it is possible to employ the shear and cell thickness necessary to test the limiting aspects of the theory. The model mesogen used in this investigation is that proposed by Gay and Berne [7]. It is described in the following section together with our model for the surface that was constructed to create the strong anchoring of the smectic layers and director implicit in the theory proposed by Mottram *et al.* [2]. The results of the simulations are given in Sec. III where they are compared with the theoretical predictions. Our conclusions are in Sec. IV.

II. SIMULATION DETAILS

The Gay-Berne generic interaction potential is well known as a powerful model for liquid crystal behavior [8] and many of the simulation details have already been reported elsewhere [9]. Here we briefly recall some basic concepts. The Gay-Berne potential is a single site or Corner potential, based on a shifted and scaled 12-6 Lennard-Jones function [7]

$$U_{GB}(R) = 4\varepsilon(\hat{\mathbf{u}}_1, \hat{\mathbf{u}}_2, \hat{\mathbf{r}})(R^{-12} - R^{-6}), \quad (2.1)$$

where

$$R = [r - \sigma(\hat{\mathbf{u}}_1, \hat{\mathbf{u}}_2, \hat{\mathbf{r}}) + \sigma_0] / \sigma_0. \quad (2.2)$$

The intermolecular contact distance $\sigma(\hat{\mathbf{u}}_1, \hat{\mathbf{u}}_2, \hat{\mathbf{r}})$ and the well depth $\varepsilon(\hat{\mathbf{u}}_1, \hat{\mathbf{u}}_2, \hat{\mathbf{r}})$ depend on the three invariants $\hat{\mathbf{u}}_1 \cdot \hat{\mathbf{u}}_2$, $\hat{\mathbf{u}}_1 \cdot \hat{\mathbf{r}}$ and $\hat{\mathbf{u}}_2 \cdot \hat{\mathbf{r}}$, where $\hat{\mathbf{u}}_1$ and $\hat{\mathbf{u}}_2$ are, respectively, the orientation vectors of the two molecules, and $\hat{\mathbf{r}}$ is the intermolecular vector. The contact distance and the well depth depend on four parameters: κ , which is a measure of the shape anisotropy; κ' , which reflects the anisotropy of the well depth, together with μ and ν , which influence the orientational dependence of the well depth. The code $GB(\kappa, \kappa', \mu, \nu)$ has been proposed [8] to distinguish between the strictly infinite

set of parameterizations of the Gay-Berne potential. The fact that there is an infinite set of Gay-Berne mesogens is, of course, a strength of the model, and enables it to describe, in a generic sense, the ever growing number of real mesogens. Two further parameters, σ_0 and ε_0 , are used to scale the distance and energy, respectively, they correspond to the contact distance σ_0 and well depth ε_0 when the two molecules are in the cross configuration, where the molecules are orthogonal to each other and to the intermolecular vector. The particular system studied here is the Gay-Berne mesogen GB(4.4, 20.0, 1, 1), which has been characterized in detail by Bates and Luckhurst [9]. This system exhibits isotropic, nematic, smectic A, smectic B, and crystal phases. The simulations have been performed at constant volume, in order to facilitate comparison with the theory of Mottram *et al.* [2]. The simulations were carried out at a scaled temperature, T^* ($\equiv k_B T / \varepsilon_0$), of 1.400 and a scaled number density, ρ^* ($\equiv \rho \sigma_0^3$), of 0.2011; at this state point the system exhibits a smectic-A phase [9,8]. The simulation box has been prepared with periodic boundary conditions in the x and y directions; the two surfaces have been placed at positions $\pm z_{\text{box}}^*$ on the z axis, parallel to the x - y plane. This geometry mirrors exactly that of the system used in the theory of Ref. [2], except in that the infinite geometry in the x and y directions is replaced, of necessity for a simulation, by periodic boundary conditions.

The theoretical model [2] requires a strong surface anchoring condition, for both the orientational and the translational degrees of freedom. It is this strong anchoring condition that compels the smectic sample to follow the movement of the surface. We model the strong translational anchoring condition by providing a modulated surface potential, along the direction of alignment of the particles, with the same periodicity d^* as that of the bulk smectic structure. The surface was built simply by placing identical Gay-Berne particles on a bidimensional rectangular grid in the x - y plane. There are six rows of particles separated by a scaled distance of 3.85 along the x direction and by a scaled distance of 0.80 in the y direction. The value of 3.85 was chosen because it corresponds to the layer spacing in the bulk smectic-A phase of GB(4.4,20.0,1,1) at the same state point as that used in our simulations of a thin film [8]. Since the position of the Gay-Berne particles constituting the surface are fixed we do not need to include their interactions with each other, however they do interact with the particles in the bulk phase.

To illustrate the principal features of this surface-particle interaction we show in Fig. 2 the energy contours for a single Gay-Berne particle as it moves over the surface. To simplify this representation the symmetry axis of the particle is held parallel to those of the particles constituting the surface; that is parallel to the easy axis as expected for particles in the bulk liquid crystal sample. In addition, the y coordinate of the particle was always kept at the same value as that for one of the particles constituting the surface. We see immediately from the contour plots in Fig. 2 that there are deep potential wells when the particle is above the center of a row of particle in the surface. Then, as it is moved from row to row along the x axis the energy increases to a maximum when it is midway between two rows. The change in the scaled en-

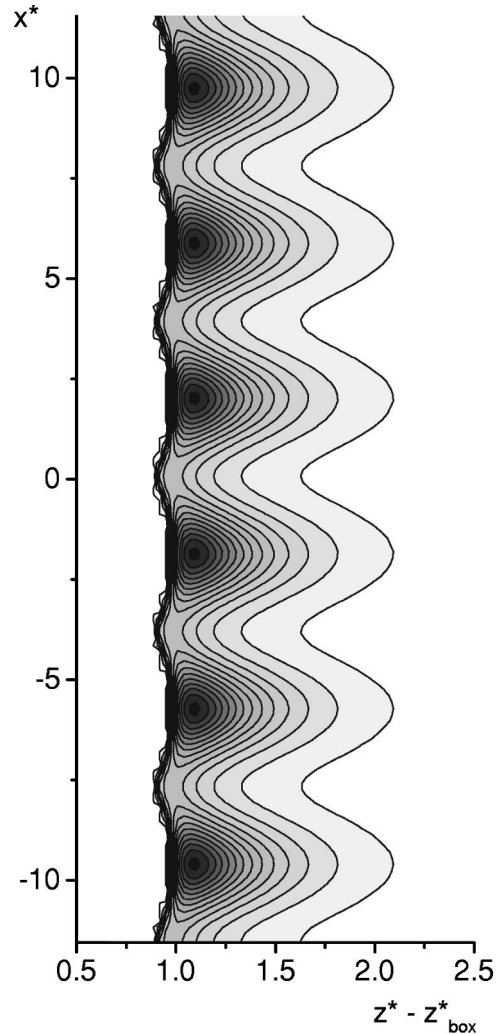


FIG. 2. Energy contours of a Gay-Berne particle interacting with the surface. The particle is confined in the x - z plane above the center of a line of particles in the surface and with its symmetry axis parallel to those of the particles defining the surface.

ergy from the minimum to the maximum is about -3.8 which is significant in comparison with the thermal energy at the scaled temperature for which the system was studied. This difference in energy is clearly what is needed to pin the smectic layers in the phase held between the two surfaces, and assumed in the mean field theory developed by Mottram *et al.* [2]. Since the surface-particle potential extends only over one molecular width at the surface, the pinning of the smectic layer is only likely to occur at the surface as required in the theory; in addition the surface is unlikely to modify the structure of the confined bulk smectic phase.

In contrast to the behavior as the particle is moved between the rows in the x direction, if it is held above the center of a given row and moved along it, that is in the y direction, then there is only a small oscillation in the well depth, with a period of 0.80, corresponding to a maximum when the particle is between two particles in a surface row and a minimum when it is above a particle. The difference in the energy is only about -0.5 and so it is not expected to have any significant influence on the ordering within a smec-

tic layer; as we shall see this is confirmed by the simulations.

Finally, as a general comment on the potential structure, we note that the width of the surface-particle interaction potential is about the same as that of the pairwise particle interaction. With the exception of the thinnest systems, this surface-particle interaction is expected to have little direct effect on the structure of the bulk mesogen in the cells we have investigated, which have a scaled width, L_z^* , up to 35. To investigate this assertion we have determined the radial distribution function, $g(r^*)$, that represents the probability of a particle being at a distance r^* from another at the origin irrespective of their orientations and that of the interparticle vector. We shall give the results for this quantity and its analog, $g_{\perp}(r_{\perp}^*)$, for the separation resolved orthogonal to the director, in the following section where we discuss their significance for the phase structure.

The simulation box contained 2000 particles, excluding those forming the two surfaces, and the scaled distance between these, L_z^* , was varied while keeping the density constant. This variation in L_z^* can only be achieved indirectly because the dimension along the x axis is determined by the number of layers, which is fixed at six. Accordingly it is the length L_y^* that can be changed but only by adding or subtracting an integer number of particles from each row defining the surface. The distance between the surfaces, given the intrinsic thickness of the Gay-Berne particles representing the surface, is actually $2z_{\text{box}}^* - 1$. The simulations have been performed by equilibrating the sample for 150 000 cycles with the rows of particles on the opposite surfaces matching perfectly. Then one surface was shifted with respect to the other the resulting degree of mismatch between the two surfaces is denoted by X_{disp}^* that is equal to x_{disp}^*/d^* where x_{disp}^* is the displacement distance of one surface with respect to the other. The initial value for X_{disp}^* was 0.1 and the system was equilibrated, again for 150 000 cycles. As we shall see the smectic layers in the bulk are found to tilt and to follow the displacement of the surface. This procedure was repeated until we observed that the smectic layers melt locally and slip back to a structure with a smaller tilt angle. Then, starting from the last unslipped configuration, the surface was shifted by a smaller amount, namely, X_{disp}^* of 0.05 and the procedure was repeated. In this way we are able to evaluate the critical degree of row mismatch, just before part of the smectic layers melt, with an accuracy of 0.025.

III. RESULTS AND DISCUSSION

We start the analysis of the results by discussing first the case for a sample having a cell thickness L_z^* of 26.91 that can be taken as being representative of thick samples, where the effect of the surfaces on the bulk structure is negligible. We present the results for the static properties in Sec. III A and give a qualitative discussion of the pseudodynamics of the slippage process in Sec. III B. The dependence of the critical deformation on the cell thickness is discussed in Sec. III C. Section III D is devoted to the description of the behavior of the thin samples, where the surfaces have a much stronger effect on the structure of the bulk smectic-A phase.

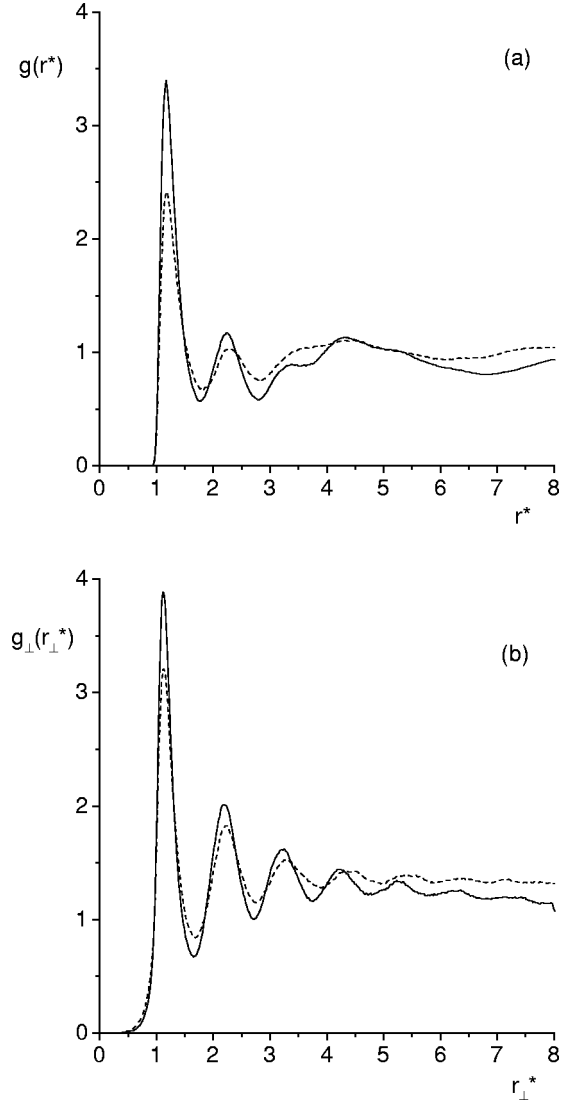


FIG. 3. The pair distribution functions for the mesogen GB(4.4,20.0,1,1) at a scaled temperature of 1.400 and a scaled density of 0.2011. (a) The radial distribution function, $g(r^*)$, and (b) the perpendicular distribution function, $g_{\perp}(r_{\perp}^*)$. The solid line shows the results for the sample in the cell with a scaled thickness of 26.91 and the dashed line is for a sample with full periodic boundary conditions.

Also, in Sec. III D, we describe some peculiar features of the unstressed samples for various thicknesses; that is, for the thickest cells a chevron structure seems to be formed that is not present in the other cases. Possible reasons for its formation are discussed.

A. Thick sample: Static

To investigate the extent to which the structure of the phase was changed by the surface, we have determined the radial distribution function $g(r^*)$. This distribution is shown in Fig. 3(a) as the solid line, for the sample with a thickness L_z^* of 26.91. The shape of the radial distribution function is typical of rodlike particles in a smectic-A phase: the first peak has a height of about 3, corresponding to the first shell

of particles at a scaled distance r^* of 1.17 and a second smaller peak at a scaled distance of 2.25 corresponding to the second shell of particles within the layer. For comparison, the radial distribution function for this Gay-Berne mesogen at a scaled temperature of 1.400 and a scaled density of 0.2011, for a sample with full periodic boundary conditions is shown as the dashed line. It appears, from the lower intensity of the first and second peaks, that the surfaces do have some effect on the properties of the sample, which does seem to be more ordered in the cell than in the bulk system with full periodic boundary conditions, as might have been expected. However, it is important to note that the surfaces do not induce a transition to a smectic- B phase. This retention of the smectic- A phase is apparent because the pair distribution function for a smectic- B phase has the first peak with a much higher intensity, of about 5 or larger, depending on the temperature [9], and the second peak is often resolved into a doublet characteristic of the hexagonal packing of the particles in the smectic layer. The splitting of the second peak into a doublet for a smectic- B phase would be even more evident for the perpendicular radial distribution function, $g_{\perp}(r_{\perp}^*)$, where r_{\perp}^* is the separation between a pair of particles resolved onto a plane orthogonal to the director. The absence of such a splitting is apparent from Fig. 3(b) and it is clear that both samples, namely, that in the cell with a thickness of 26.91 (solid line) and that in the box with full periodic boundary conditions (dashed line), correspond to a smectic- A phase. There is, however, a small difference between $g_{\perp}(r_{\perp}^*)$ for these two systems that again indicates the somewhat enhanced order resulting from the surface interactions.

An alternative view of the structure within the smectic layers can be obtained from the singlet translational distribution function, $\rho(x^*, z^*)$, which gives the probability of finding a particle at a position (x^*, z^*) irrespective of the y^* coordinate and the orientation of the particle. This distribution function has the advantage of revealing how the structure within a layer varies with the distance from the surface. The distributions were obtained as averages over 10 000 configurations each separated by 2 cycles for a production run of 20 000 cycles, following an equilibration run of 150 000 cycles. The contour plot for $\rho(x^*, z^*)$ shown in Fig. 4(a) corresponds to the unstressed sample, where the rows of particles composing the surfaces are perfectly matched, as indicated by the numbers labeling the row positions on the two surfaces. The results in Fig. 4(b) are for the sample with the highest surface stress, before slippage occurs, at this point the surfaces have a mismatch, X_{disp}^* , of 1.950, which corresponds to essentially two layers. An additional relative movement of $0.025d^*$ of the surfaces results in the melting of part of the layers that then slip back and rejoin to form a configuration with a smaller mismatch of 0.975, that is almost one layer. The translational distribution function $\rho(x^*, z^*)$ for this final slipped configuration is shown in Fig. 4(c) and the labeling of the surface sites of the rows indicates the change in the structure; thus the layer joining the surface at the positions labeled (1) on the left and right hand side in

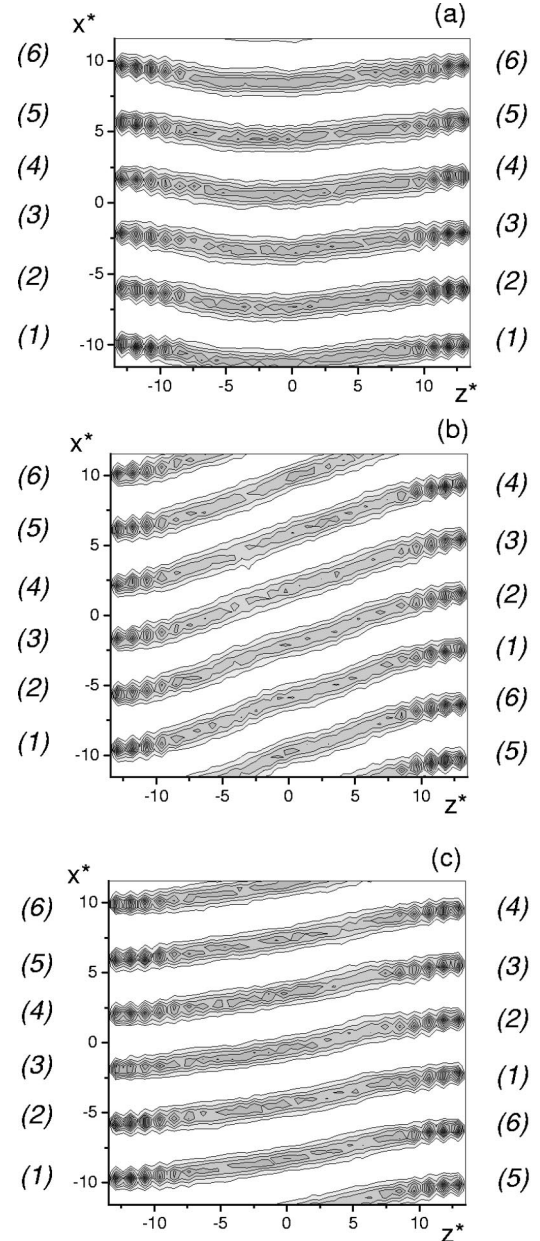


FIG. 4. The contour plot for the singlet translational distribution function of the center of mass, $\rho(x^*, z^*)$, for the sample with a thickness L_z^* of 26.91 at different surface mismatches X_{disp}^* : (a) 0.0; (b) 1.950, before the slippage occurs; and (c) 0.975, after the slippage; the critical mismatch X_{disp}^{c*} , is 1.9625 ± 0.0125 . The numbers in parenthesis on the surfaces at either side label the surface sites at which the smectic layers are anchored.

Figs. 4(a) and 4(b) now join the position labeled (6) on the right hand surface in Fig. 4(c).

A chevron structure is clearly evident in Fig. 4(a), that is, the layers do not pass from one surface to the other in a straight line but they are slightly bent. We shall return to this point in Sec. III D. It is also worth mentioning that the translational order within the layers close to the surfaces appears to be quite different to that in the bulk. This ordering is indicated by the peaks in the singlet distribution function $\rho(x^*, z^*)$ in the vicinity of the surfaces. This effect is clearly

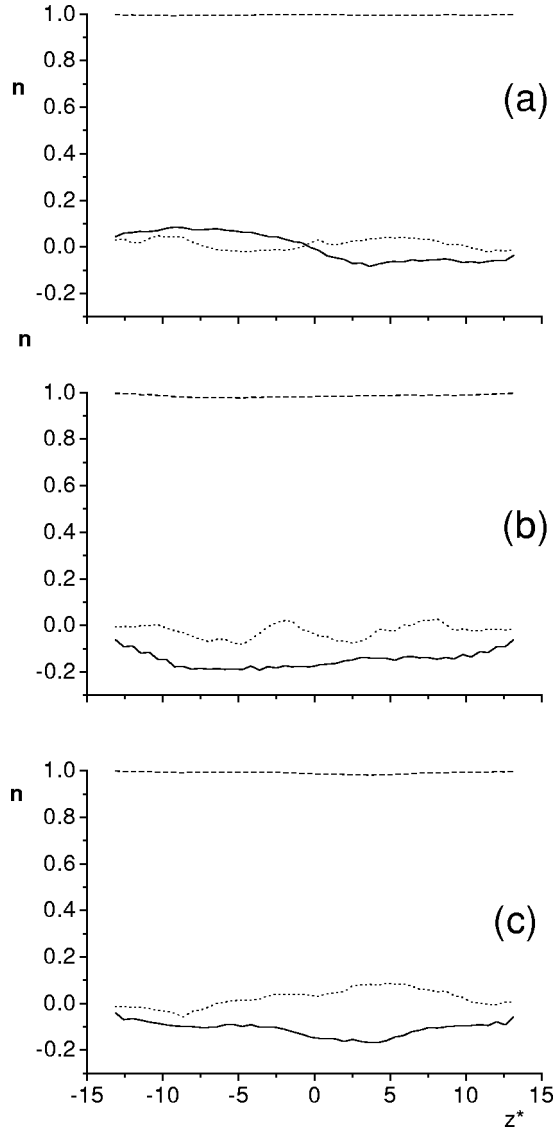


FIG. 5. The director components n_x (dashed), n_y (dot), and n_z (solid), for the sample with a thickness L_z^* of 26.91 at various surface mismatches, X_{disp}^* : (a) 0.0; (b) 1.950, before the slippage occurs; and (c) 0.975, after the slippage; the critical mismatch, X_{disp}^{c*} , is 1.9625 ± 0.0125 .

related to the highly localized attraction between the surface and the particles within the smectic layer, that is the strong anchoring condition we have described previously. However, the additional translational order does not extend far into the smectic layer that retains its disordered structure in the bulk. In other words the surface interaction has not changed the global structure within the smectic layers and the phase remains a smectic *A* as we had anticipated.

We now consider the director orientation and how this changes as the sample is sheared. In Fig. 5 we show the components of the director, n_x , n_y , and n_z with respect to the laboratory frame (see Fig. 1) as a function of the position along the z axis, that is, on going from one surface to the other, for (a) the unshereed configuration, (b) the configuration just before the layers have melted locally, and (c) for the configuration after the layers have melted and reformed. The

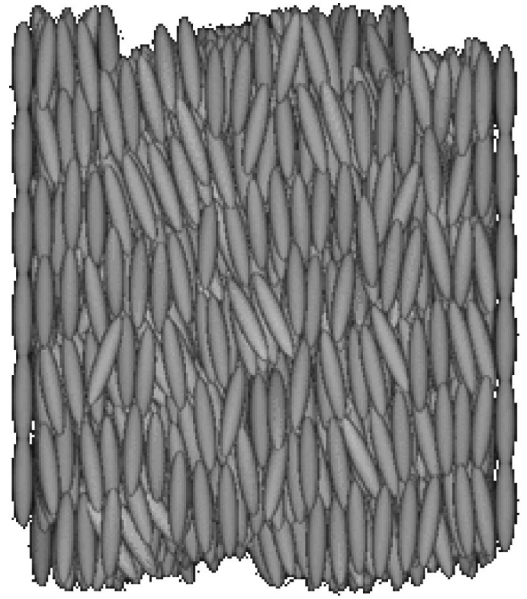


FIG. 6. A snapshot showing particles of the sample in a cell with a scaled thickness of 26.91 and a mismatch, X_{disp}^* of 1.950 viewed along the y direction.

n_x component of the director is seen to be essentially equal to unity across the entire cell confirming the expected alignment parallel to the easy axis. However, we should note that n_x is not particularly sensitive to deviations of the director away from the easy axis. This insensitivity is not the case for the z component of \mathbf{n} ; in fact the n_z component for the unshereed sample does show a change, on going from one surface to the other from a positive value slightly larger than 0.1, through 0 in the center of the cell to a negative value of about -0.1 . In contrast the n_y component essentially fluctuates about zero. This behavior corresponds to a change in the tilt of the director in the x - z plane and is related with the chevron structure observed for the unshereed system. The tilt of the director is associated with the bend of the layers in order that the particles remain, on average, perpendicular to the layers, as in an unperturbed smectic-*A* phase. The variation of the n_z component across the cell changes as the system is sheared [see Figs. 5(b) and 5(c)] becoming more symmetric and negative. This change in n_z means that the weak chevron structure observed for the unshereed sample is soon lost and the particles in the center of the cell tilt in association with the layers in order to remain perpendicular to them. As we can see in Figs. 5(b) and 5(c) the n_z component is now negative across the entire cell, corresponding to the particles being perpendicular to the tilted layers, as shown in Figs. 4(b) and 4(c). In Fig. 6 we show a snapshot taken of the sample for a mismatch X_{disp}^* of 1.950 with the particles represented as ellipsoids of revolution, consistent with the shape of a Gay-Berne particle; the tilt of the layers with respect to the surfaces and also the tilt of the particles, in the middle of the cell, to orient more or less perpendicular to the layers are clearly visible. A tilt of the particles adjacent to the surface is also apparent but this tilt is significantly smaller than for those at the center of the cell, in keeping with the smaller tilt of the layers at the surface (see Fig. 4).

The orientational and translational order of the smectic-A phase can be characterized by the order parameters, η and τ , respectively. These order parameters are defined as the averages

$$\eta = \langle (3 \cos^2 \beta - 1)/2 \rangle, \quad (3.1)$$

where β is the angle between the molecular symmetry axis and the director and

$$\tau = \langle \cos 2\pi x/d \rangle, \quad (3.2)$$

where x is the distance of the particle from the center of the layer. Within the Monte Carlo simulation the orientational order parameter was evaluated via the \mathbf{Q} tensor for particles in 20 slices taken across the cell. It was averaged over 10 000 configurations each separated by two cycles and then diagonalized; the largest eigenvalue gives the orientational order parameter η and the eigenvector associated with this eigenvalue gives the director orientation. The determination of the translational order parameter τ is not so straightforward or precise. It was achieved via the relationship

$$\tau = \left| \int_{-x_{\text{box}}^*}^{+x_{\text{box}}^*} \rho(x^*) \exp(i2\pi x^*/d^*) dx^* \right|, \quad (3.3)$$

where the singlet translational distribution function, $\rho(x^*)$, gives the probability of finding a particle at position x^* . This result would be exact if the layer normal was parallel to the x axis. The alignment of the layer normal does not occur for the sheared samples but because we are interested in τ for thin slices taken across the cell the error introduced is small. In fact the tilt of the layers corresponds to a slight broadening of the distribution function and hence a small reduction in τ . The orientational, η , and translational, τ , order parameters are shown, as a function of the position across the cell, in Figs. 7(a)–7(c) for the same surface mismatch of the system as those in Fig. 5. The orientational order parameter shows a slight alternation in value close to the surface, caused presumably by the density modulation induced by the strong anchoring condition. Comparing Figs. 7(a)–7(c) with the corresponding panels in Fig. 4 reveals that where the density is higher the orientational order is also slightly higher. However, it levels off rapidly to a relatively high value of about 0.90 in the bulk of the sample without showing any modulation, in keeping with the assumption that surface effects are not transmitted far into the bulk. The translational order parameter shows a similar behavior, that is, for the unsheared sample, it is high at the surface, about 0.80, and then decreases to about 0.65 in the bulk. There is also a slight modulation in the translational order close to the surface. The order parameter, τ , decreases slightly when the sample is highly sheared, as the results in Fig. 7(b) demonstrate for a mismatch between the surfaces of 1.950; although in some regions of the sample it can be as low as 0.5. In contrast the orientational order parameter does not show any significant change. When the system relaxes back to a mismatch, X_{disp}^* , of 0.975 the translational order parameter increases approaching the value for the unsheared cell and, as expected, the orientational order parameter is essentially unaltered.

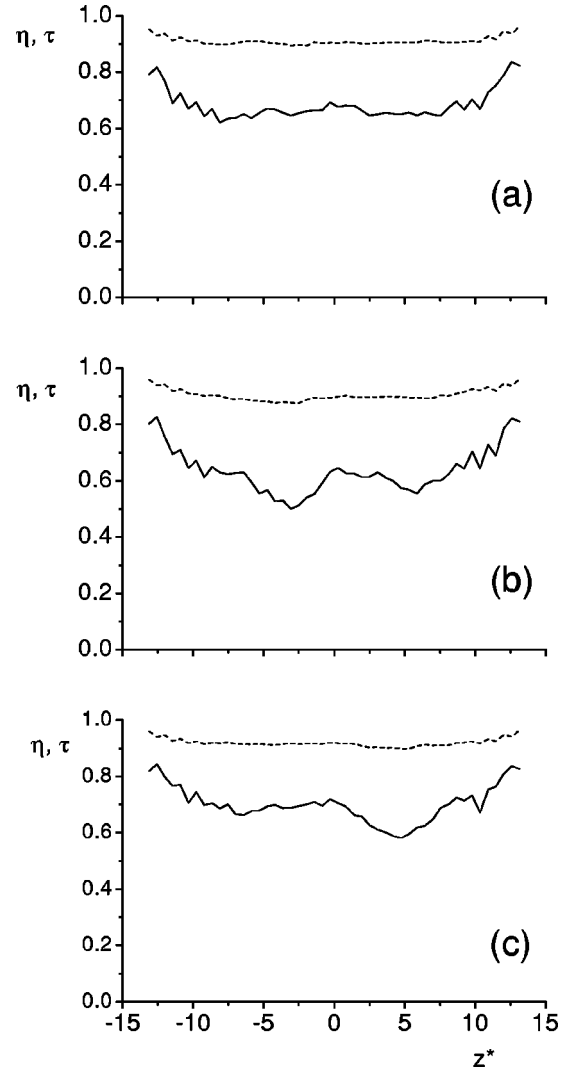


FIG. 7. The orientational η (dashed), and translational τ (solid) order parameters as a function of the position in the cell for the sample with a thickness L_z^* of 26.91 at different surface mismatch X_{disp}^* : (a) 0.0; (b) 1.950, before the slippage occurs; and (c) 0.975, after the slippage; the critical mismatch X_{disp}^{c*} is 1.9625 ± 0.0125 .

B. Thick sample: Pseudodynamics

Since we are able to prepare the state in which the mismatch has just passed its critical value it should be possible to monitor the process by which the system passes to a metastable supersheared state. In principle, this nonequilibrium process can be followed by a molecular dynamics simulation. In practice such a simulation may take an impossibly long time to achieve and an alternative is to use a Monte Carlo simulation in which the configurations are linked by steps that mimic dynamic changes, at the molecular level, occurring in a real system [10]. In fact such Monte Carlo simulations have been used to investigate the diffusion and annihilation of defects in a lattice model of a nematic [11]. We have also shown that for the field induced alignment of the nematic phase formed by the Gay-Berne mesogen GB(4.4,20.0,1,1) the number of cycles is proportional to time [12]. As our primary interest is in the structure of the stable

and metastable states for a smectic-*A* phase subject to shear, we have used the Monte Carlo technique. We have, therefore, configurations showing how the structure of the sheared smectic-*A* phase changes as it passes from the unstable to the metastable state and these should provide an indication, at least, as to how the system evolves during this change.

Here we consider this pseudodynamic process for the thick sample with L_z^* of 26.91. We shall illustrate the changes first as a series of snapshots taken during the passage of the sheared smectic-*A* phase between the two states with their different layer tilts. In the snapshots, shown in Fig. 8, the particles are represented simply as circles located at their centers of mass to demonstrate the translational order more clearly, although all information relative to the orientational order is necessarily removed. The Monte Carlo simulations start from a sample equilibrated with a relative mismatch, X_{disp}^* , of 1.950 and then with one surface having been moved by a further $0.025d^*$ to reach a value of X_{disp}^* above its critical value. The initial configuration shows the layers intact in the supersheared unstable state although the translational order is clearly significantly weaker for the regions of the layers in the center of the cell in comparison with those at the surface. After 34 000 cycles [see Fig. 8(b)] the layer structure has not changed to any significant extent and this is also true after a further 5000 cycles. However, after 44 500 cycles [see Figs. 8(d)] it is apparent that the translational order for all the layers is being reduced significantly in a relatively narrow region near to the center of the cell. In addition to this loss of order the layers originating from one side of the cell appear to terminate at a position midway between those layers coming from the other side. The reduction of the translational order localized in this region continues, as is clear from the snapshots taken after 45 500 and 46 000 cycles [see Figs. 8(e) and 8(f)]. The translational order then begins to rebuild in regions adjacent to the existing layers, as we can see after 48 000 and 49 000 cycles [see Figs. 8(g) and 8(h)]. As the order is reestablished at these positions so they link together the layers attached to either side of the cell in such a way that the mismatch is reduced by one layer. After 57 000 cycles this process of rebuilding the complete layers is still occurring but after a further 10 000 cycles it is complete [see Fig. 8(j)]. It is also apparent that the translational order in the rebuilt layers of the metastable supersheared state is significantly higher than in the unstable supersheared state, as we might have anticipated.

To characterize the slippage process more quantitatively we have also calculated the translational order parameter, τ , for slices across the cell and their variation with the number of cycles is shown in Fig. 9. The results were calculated after dividing the box into ten slices parallel to the surfaces; they are labeled (a) to (j) in the figures from the left to the right hand surface. Since it is not possible to calculate the singlet translational distribution function, $\rho(x^*)$, at each cycle with a good signal-to-noise ratio the translational order parameter was calculated directly from its real, Re , and imaginary, Im , parts, which were evaluated as averages over the particles in each slice,

$$\text{Re}(\tau) = \langle \cos 2\pi x^*/d^* \rangle, \quad (3.4)$$

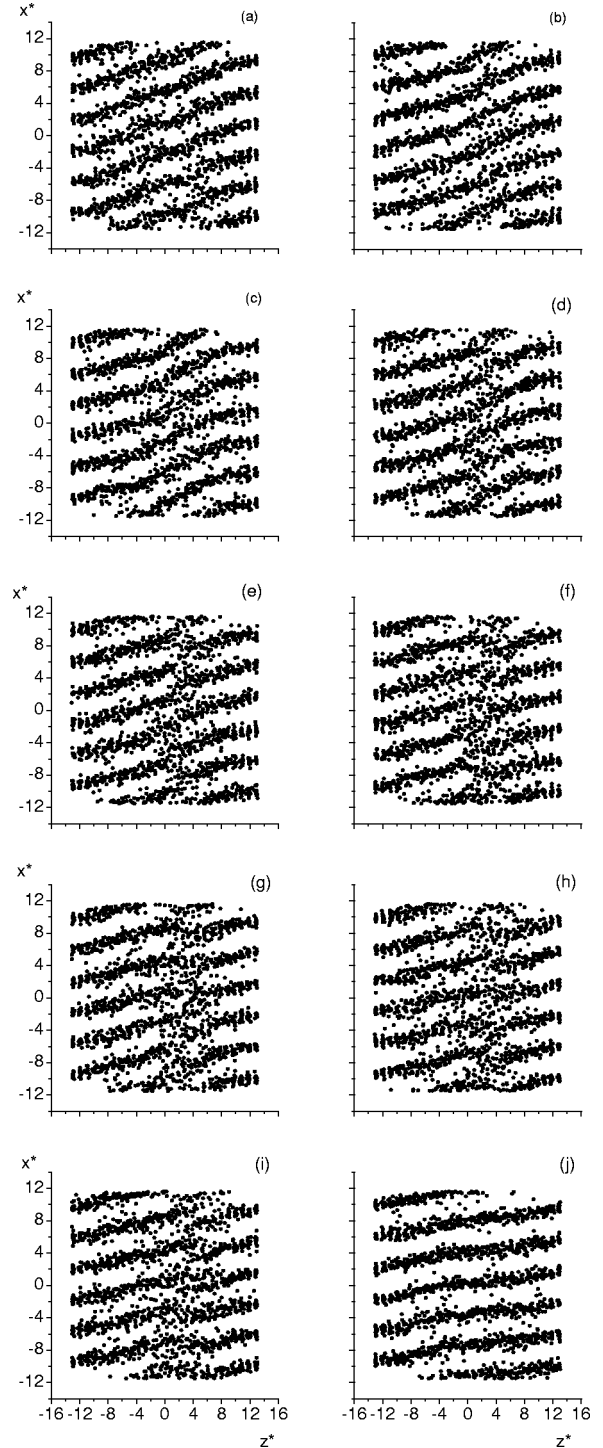


FIG. 8. Pseudodynamics of the slippage process for the thick sample (L_z^* of 26.91). The starting configuration is obtained from the equilibrated sample with a surface mismatch, X_{disp}^* of 1.950, and then increasing the mismatch by an additional 0.025 into the unstable supersheared state. (a) start; (b) cycle 34 000; (c) cycle 39 000; (d) cycle 44 500; (e) cycle 45 500; (f) cycle 46 000; (g) cycle 48 000; (h) cycle 49 000; (i) cycle 52 000; (j) cycle 67 000.

$$\text{Im}(\tau) = \langle \sin 2\pi x^*/d^* \rangle, \quad (3.5)$$

$$\tau = \sqrt{\text{Re}(\tau)^2 + \text{Im}(\tau)^2}. \quad (3.6)$$

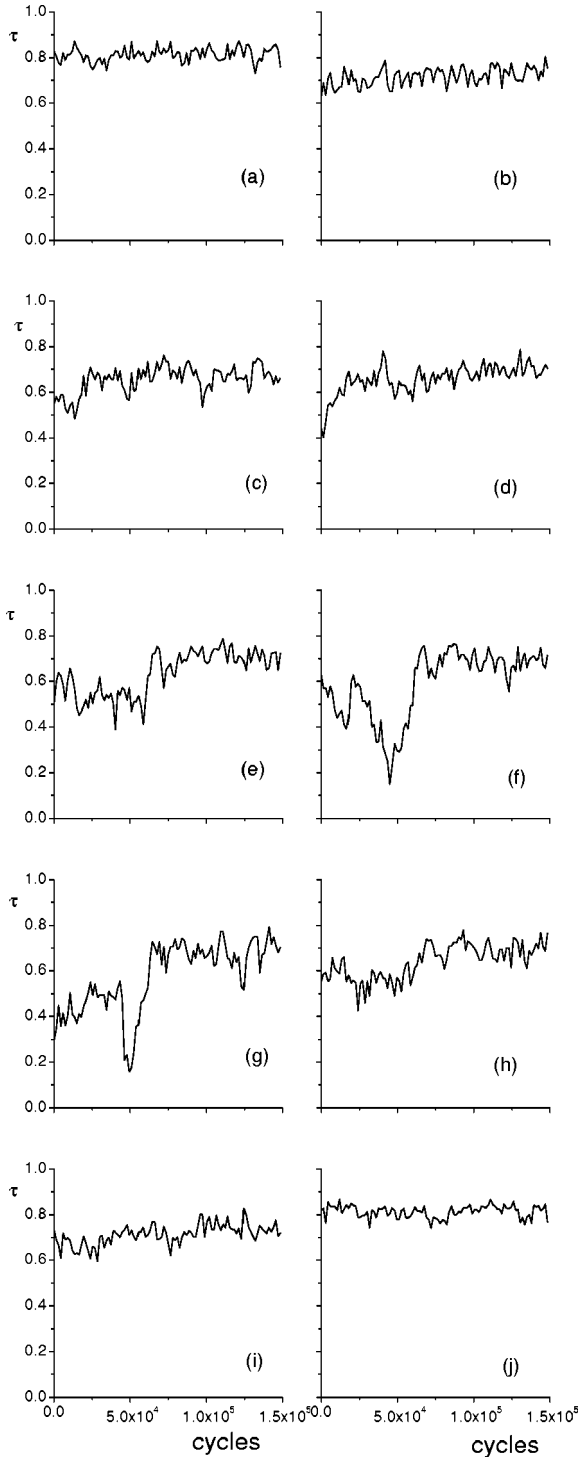


FIG. 9. The translational order parameter, τ , as a function of the number of cycles during the slippage process calculated in 10 equally spaced slices [(a) to (j)] parallel to the x - y plane.

The translational order parameter at the start of the simulation adjacent to the surface is high, approximately 0.8, and then decreases in the center of the cell, although the smallest value of about 0.4 occurs for slices on either side of the center. This variation of the translational order parameter is consistent with the snapshot in Fig. 8(a), taken of the unstable supersheared state. During the passage to the meta-

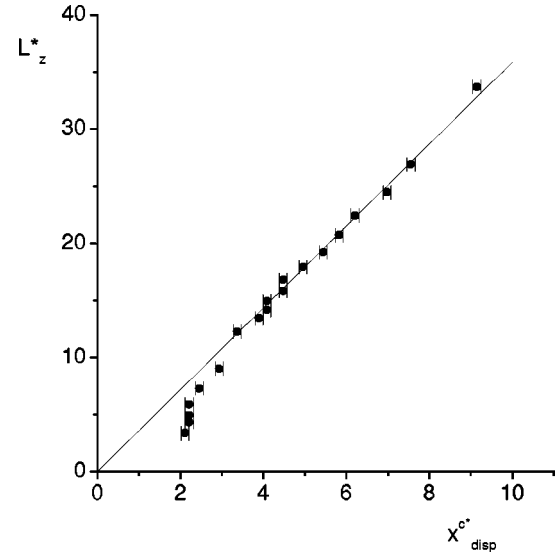


FIG. 10. The dependence of the critical relative displacement, x_{disp}^{c*} , on the cell thickness L_z^* . The solid circles are the results of the simulation and the solid line is the best linear fit to the data, excluding the five points for the thinnest samples.

stable supersheared state it is of interest to note that the translational order parameter for the slices adjacent to the surfaces [see Figs. 9(a) and 9(j)] as well as their neighboring slices [see Figs. 9(b) and 9(i)] do not change. This constancy of the translational order presumably results from the interaction with the surface and the fact that near the surface the smectic layers are not significantly tilted. In contrast, for slices six and seven, in Figs. 9(f) and 9(g), respectively, the translational order parameter decreases suddenly and significantly after approximately 45 000 cycles; for these slices it falls to approximately 0.1 before increasing significantly to a value of about 0.7. This sudden change in the translational order parameter takes place over about 25 000 cycles and corresponds to a localized melting of the smectic-A phase. Subsequently there is a slow increase in the translational order parameter that appears to reach a limiting value after about 75 000 cycles, in agreement with the snapshots in Fig. 8.

It appears, therefore, that the layers melt at some point near the center of the cell, then they move coherently, with a local reduction of the translational order, to rejoin after a shift equal to the layer periodicity. This process of layer reformation is also evident in the snapshots in Fig. 8 where the layers appear almost intact except, of course, in the region where the melting has occurred. The intermediate structure [see Figs. 8(e) and 8(f)] is characterized by layers that are mismatched by half the layer periodicity d^* near the center of the cell.

C. Thickness dependence

In Fig. 10 we report the dependence of the critical relative displacement, x_{disp}^{c*} , on the cell thickness, L_z^* . For each thick-

ness, x_{disp}^{c*} has been calculated as the average between the largest displacement for which the layers do not slip back and the smallest displacement for which the layers do slip back. Since they differ by $0.025d^*$, this has been taken as an indication of the total error range of the critical mismatch. We have observed, in the preceding section, that the slippage process, when it does occur, takes place in a few tens of thousands of cycles; therefore, the equilibration run of 150 000 cycles certainly appears to be sufficient to investigate the process, that is, it is unlikely that the slippage does not occur in the simulation once the displacement has exceeded its critical value. The cell thickness, L_z^* , and the critical displacement, x_{disp}^{c*} , show a linear dependence until a critical scaled cell thickness is reached of about 5. From the slope of the fitted curve (the best fit is shown as the solid line in Fig. 10) we can estimate that this corresponds to a tilt defined as $\tan^{-1}(x_{\text{disp}}^{c*}/L_z^*)$, with respect to the surface normal, of 15.5° . This tilt angle, which is a purely geometric parameter of the experiment should not be confused with the tilt of the smectic layers that, as we can see from Fig. 4 and Fig. 8, varies across the cell. At the surface the layer tilt will be less than 15.5° whereas in the center of the cell it will be greater. When the thickness of the cell becomes too small then a deviation from linearity is necessarily observed and the data points do not lay on the line through the origin. This is expected when the cell thickness becomes comparable to the layer spacing: it is not possible to induce a slippage of the layer by an amount equal to the smectic periodicity d^* when the mismatch is smaller than $d^*/2$. This is indeed the limiting value where the data points converge.

The slope of the linear region of the $x_{\text{disp}}^{c*} - L_z^*$ plot allows us to make a more quantitative contact with the mean field theory developed by Mottram *et al.* [2]. In this the fundamental length scale, ξ , is defined as

$$\xi = (\zeta_{\perp} / |a|) \quad (3.7)$$

and measures the distance over which changes in the smectic order are expected to occur. In this expression a is a coefficient for the quadratic term in the free energy depending on the translational order parameter; ζ_{\perp} is the coefficient controlling the departure of the director from the layer normal. Numerical evaluation of the mean field free energy for the system yields, implicitly, the slope of the $x_{\text{disp}}^{c*} - L_z^*$ plot in terms of ξ . Comparing this predicted value with that obtained from the simulation yields a value for ξ of just $1.2\sigma_0$. This result for the relaxation length characterizing fluctuations in the smectic order may appear to be somewhat small corresponding as it does to just one molecule. Presumably the shortness of ξ is related to the strong side-by-side attractions of the Gay-Berne particles. Indeed, the radial distribution function $g(r^*)$ and the perpendicular distribution function $g_{\perp}(r_{\perp}^*)$, shown in Fig. 3, do show a strong first neighbor peak occurring almost at the same distance of $1.2\sigma_0$. Therefore, the relaxation length ξ seems to be related with the order within the smectic layer, which is very short range for the smectic-A phase.

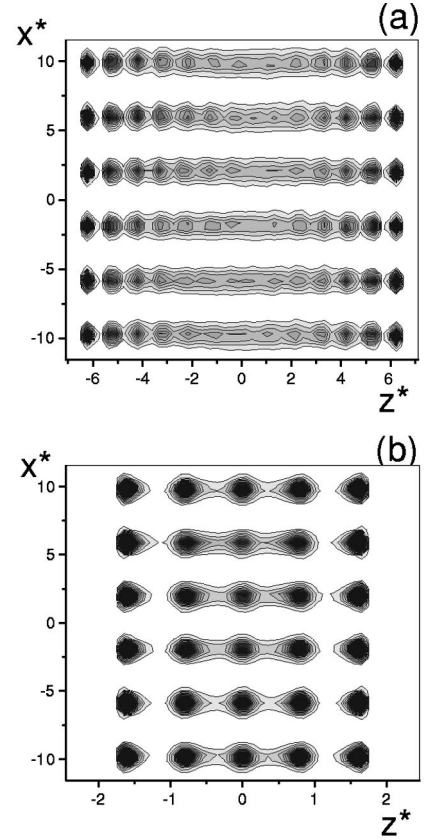


FIG. 11. The contour plot showing the singlet translational distribution function, $\rho(x^*, z^*)$, for the sample with a cell thickness, L_z^* , of (a) 14.20 and (b) 4.90.

D. Thin sample

In Fig. 11 we show the singlet distribution function, $\rho(x^*, z^*)$, for samples with cell thickness, L_z^* , of 14.20 (a) and 4.90 (b). In these two cases we observe relatively larger spatial variations in the density within the layers. For the thinner sample the continuum description of the smectic-A phase clearly no longer holds. The surfaces are only a few molecular diameters apart and since the correlation length for the surface-induced structure seems to be independent of the sample thickness and equal to a few molecular dimensions (see Figs. 4, 8, and 11) the surface-induced translational ordering perpendicular to the surface now extends over the entire cell. Nevertheless, it is still possible to measure a critical relative displacement for the layer slippage. We also notice that the chevron structure, which was present for the unstressed sample with the thick cell (L_z^* of 26.91) has vanished for the thinner cells. The reason for the formation of the chevron structure is probably due to the effect of the surfaces that induce a strong translational ordering in the smectic-A layers within their vicinity; in turn, this change of structure alters the smectic periodicity, for this region of the smectic layers, with respect to that for the bulk sample. However, the effect is lost when the surfaces are mismatched and is evident only for the thicker sample.

IV. CONCLUSIONS

In this paper we have presented the results of a computer simulation investigation of a smectic-*A* liquid crystal placed in a cell in which the walls are subject to an increasing shear. We have studied the process of layer slippage for this sample, and compared the results to the rather extensive mean field theory proposed by Mottram *et al.* [2]. Their theoretical analysis requires a phenomenological parameter, ζ_{\perp} , to define the critical mismatch for thick cells. In addition it presents an unambiguous picture of the behavior of the critical shear as a function of the cell thickness. At high thickness the critical mismatch tends to increase linearly. For very thin cells, of molecular dimensions, the critical displacement is exactly half a smectic layer. Mottram *et al.* [2] predict the existence of a critical thickness below which there will be layer melting in the center of the cell.

The simulation results are clearly consistent with this picture. The linear dependence of the critical relative layer displacement on the cell thickness is verified, as is the departure from this law at low cell thickness. The thin cell result is not verified, but only because in this limit the phenomenological theory is no longer applicable since the theory assumes no additional translational ordering in a direction perpendicular to the cell walls. In contrast there is such an ordering for our model, but as we have observed only on molecular scales. Nevertheless the signature of the thin cell prediction is still present, in the form of the approach of the critical mismatch to its thick film limit.

We were also able to observe the nonequilibrium process of layer melting and subsequent reformation beyond the critical mismatch. The process is observed to take place over several thousands of Monte Carlo cycles. The translational order near the middle of the cell is reduced significantly and the layers on each side of the cell reattach to each other so as to tilt less. Initially this reattachment of the layers seems to involve some reverse layer tilt in the middle of the cell, but at a later stage this reverse tilt relaxes. Although this feature of the layer relaxation was not predicted by Mottram *et al.* [2], it is possible, with hindsight, to discern this behavior qualitatively.

The agreement between theory and simulation is remarkably good, given the extremely simplified representation of smectic layering used in the theory; this represents the periodic structure by a single complex order parameter that is likely to be reasonable when the translational order is low whereas for the Gay-Berne mesogen it is high [9]. In principle, therefore, many order parameters are needed, at least formally, to describe the periodic structure. The theory also posits strong layer anchoring at the constraining boundary plates that may not occur in real samples, but which we have nevertheless built into our computational model thus facilitating comparison with the theory. The basic conclusions of the theory are confirmed, notwithstanding the fact that for the length scales on which we have necessarily carried out our simulations, the original theoretical model is no longer strictly valid.

Despite the agreement with theory, our simulation study also raises a number of intriguing questions. First, although

Mottram *et al.* [2] presented a formal mean field theory of layer slippage, the molecular picture is far from clear. Presumably at the critical mismatch the mean field enforcing the translational order disappears. As yet there is no theory of this phenomenon, although, in principle, the smectic potential could be monitored using a computer simulation. Second, the use of a periodic potential at the wall to pin the smectic layers might well be artificial although some interaction for pinning is clearly necessary. In a Monte Carlo simulation the periodic potential, as in the mean field theory of Mottram *et al.* [2], is probably an essential precondition for the pinning of the smectic layers, we have seen, but it may not be. The crucial question concerns the fluid boundary conditions at the walls. The classical no-slip boundary conditions should enforce layer tilt, for they involve coherent surface motion and bulk motion at the surface. Layer relaxation in the absence of coherent hydrodynamic motion is very slow. The molecular basis of fluid boundary conditions is known to be a hard problem, in general, and may well be at the heart of this particular problem. The situation could be clarified by repeating these simulations with weaker or rather less direct assumptions about the nature of the pinning interaction at the boundaries. Such simulations should be supplemented by molecular dynamics simulations, in which the role of hydrodynamics would be elucidated. We note also that our simulations were performed for the significant but still possibly small number of 2000 particles. Notwithstanding the encouraging results, larger simulations would, as is invariably the case, be desirable.

Third, the problem could also be approached using simulation, but now considering layers that are adiabatically thinned. The layer-breaking instability may well be related to layer buckling instabilities at lower layer strain as predicted for a smectic-*A* phase under analogous conditions by Helfrich and Herault [13]. The idea here is that it is almost always effective for a system to localize the strain. This it will do by buckling, thus preserving the layer thickness locally [14]. In the context of this work, the buckling instability might be expected to be visible before the critical tilt as a result of the dilative strain introduced by the layer tilt.

Finally, we note that this problem is but one example of the relaxation of a smectic system, and this is subject to smectic hydrodynamics. We observe that there has been little work in general on the hydrodynamics of smectic systems [15]. The relaxation of smectic systems provides a hydrodynamic system of unparalleled complexity. The simulations presented in this paper form a first step in the investigation of this interesting and difficult general problem.

ACKNOWLEDGMENTS

We wish to thank Martin Bates (University of Southampton) for providing a copy of his Monte Carlo simulation code that was modified for this investigation. In addition we acknowledge the allocation of significant computational resources by the Southampton University Computing Service.

T.J.S. is extremely grateful to Nigel Mottram (University of Strathclyde) for long and continuing discussions on this problem. He also acknowledges an illuminating discussion with Doug Cleaver (University of Derby). He thanks Steve Elston (University of Oxford) and Mike Towler (Sharp Labo-

ratories of Europe, Oxford) for drawing his attention to the problem. G.R.L. is grateful to the EU for the award of the TMR Network Grant No. FMRX-CT97-0121 that provided, amongst other things, the financial support for G.S., who thanks G.R.L. and the TMR Network for this.

-
- [1] P.G. de Gennes and J. Prost, *The Physics of Liquid Crystals*, 2nd ed. (Oxford University Press, Oxford, 1993).
- [2] N.J. Mottram, T.J. Sluckin, S.J. Elston, and M.J. Towler, *Phys. Rev. E* **62**, 5064 (2000).
- [3] S.J. Elston and M.J. Towler, *Phys. Rev. E* **57**, 6706 (1998).
- [4] N.A. Clark and T.P. Rieker, *Phys. Rev. A* **37**, 1053 (1988).
- [5] S. Kralj and T.J. Sluckin, *Phys. Rev. E* **48**, 3244 (1993).
- [6] M. Cagnon and G. Durand, *Phys. Rev. Lett.* **70**, 2742 (1993).
- [7] J.G. Gay and B.J. Berne, *J. Chem. Phys.* **74**, 3316 (1981).
- [8] M.A. Bates and G.R. Luckhurst, *Struct. Bonding (Berlin)* **94**, 65 (1999).
- [9] M.A. Bates and G.R. Luckhurst, *J. Chem. Phys.* **110**, 7087 (1999).
- [10] A. Rey, A. Kolinski, J. Skolnik, and Y.K. Levine, *J. Chem. Phys.* **97**, 1240 (1992); Y.K. Levine, A. Kolinski, and J. Skolnik, *ibid.* **98**, 7581 (1993); D.A. van der Sijts and Y.K. Levine, *ibid.* **100**, 6783 (1994).
- [11] C. Liu and M. Muthukumar, *J. Chem. Phys.* **106**, 7822 (1997).
- [12] G.R. Luckhurst and G. Saielli (unpublished).
- [13] W. Helfrich, *Appl. Phys. Lett.* **17**, 532 (1970); J.P. Hurault, *J. Chem. Phys.* **59**, 2068 (1973).
- [14] S.J. Singer, *Phys. Rev. E* **48**, 2796 (1993).
- [15] See, e.g., H.R. Brand, P.K. Mukherjee, and H. Pleiner, *Phys. Rev. E* **63**, 061708 (2001), and references therein.